DOI: 10.1002/ejic.200900590

Syntheses and Crystal Structures of dmso-Coordinated Tungstoantimonates(III) and -bismuthates(III)

Li-Hua Bi,*[a] Guang-Feng Hou,[a] Ya-Yan Bao,[a] Bao Li,[a] Li-Xin Wu,*[a] Zhong-Min Gao[b] Timothy McCormac,[c] Sib S. Mal,[d] Michael H. Dickman,[d] and Ulrich Kortz[d]

Keywords: Dimethyl sulfoxide / Polyoxometalates / Antimony / Bismuth / Tungsten

Four new organic–inorganic hybrid compounds based on dmso-coordinated heteropolytungstates as $[Ru(bpy)_3]^{2+}$ (Rubpy) salts {$[Ru(bpy)_3]_2Na_2[Sb_2W_{22}(dmso)_4O_{72}]\cdot 4dmso\cdot 4H_2O$ (**1a**), $[Ru(bpy)_3]_2Na_2[Bi_2W_{22}(dmso)_4O_{72}]\cdot 4dmso\cdot 4H_2O$ (**2a**), $[Ru(bpy)_3]_2[Sb_2W_{20}Fe_2(dmso)_8O_{68}]\cdot 9dmso\cdot 12H_2O$ (**3a**), $[Ru(bpy)_3]_2[Bi_2W_{20}Fe_2(dmso)_8O_{68}]\cdot 9dmso\cdot 12H_2O$ (**4a**)} have been synthesized and characterized by IR spectroscopy, elemental analysis, thermogravimetry, cyclic voltammetry, X-ray powder diffraction and single-crystal X-ray diffraction. The structural analyses indicate that the dmso molecules are coordinated onto the polyanion frameworks through four W–O–$S(CH_3)_2$ bonds for **1a** and **2a**, six Fe–O–$S(CH_3)_2$ and two W–O–$S(CH_3)_2$ bonds for **3a** and **4a**. The compounds **1a**–**4a** represent novel members of dmso-coordinated tungstoantimonates and tungstobismuthates prepared by routine synthetic reactions in the mixed solutions with dmso/H_2O (1:1, v/v). The cyclic voltammetry studies of **1a**–**4a** in dmso/H_2SO_4 medium using the glassy carbon electrode as a working electrode show the respective electrochemical behaviors of the W and Ru centers within **1a** and **2a**, and the W, Fe and Ru centers within **3a** and **4a**.

Introduction

Hybrid organic–inorganic materials continue to attract attention due to the possibilities of combining the features of the organic and inorganic components to generate unusual structures, properties, or applications.[1,2] Polyoxometalates (POMs) are inorganic metal–oxygen cluster species with an enormous structural and compositional variety.[3–6] Hybrid materials containing POMs have shown exciting electronic, optical, magnetic and catalytic properties, which make POMs attractive inorganic candidates.[7–9] Therefore, the design of new molecular hybrid materials containing POMs as building blocks constitutes an interesting research area.

The existence of Sb^{III}- and Bi^{III}-containing POMs has been known for several years. The lone pair of electrons on the hetero atom does not allow the closed Keggin unit to form, which has resulted in some unexpected structures, for example $[NaSb_9W_{21}O_{86}]^{18-}$, $[Na_2Sb_8W_{36}O_{132}(H_2O)_4]^{22-}$.[10,11] The polyoxoanions $[XW_9O_{33}]^{9-}$ (X = Sb^{III}, Bi^{III}) and $[X_2W_{22}O_{74}(OH)_2]^{12-}$ (X_2W_{22}) (X = Sb^{III}, Bi^{III}) are probably the mostly studied systems in the Sb^{III}- and Bi^{III}-containing POMs.[12–15] Up to now, the compounds $[M_2(H_2O)_6(WO_2)_2(\beta\text{-}XW_9O_{33})_2]^{(14-2n)-}$ ($X_2W_{20}M_2$) (X = Sb^{III}, Bi^{III}; M^{n+} = V^{4+}, Fe^{3+}, Co^{2+}, Mn^{2+}, Ni^{2+}, Cu^{2+}, Zn^{2+}) have been reported.[11,16] More recently, our group presented a one-dimensional chain-like Cd^{II}-substituted tungstoantimonate $[Sb_2W_{21}Cd(OH)_2O_{73}]^{14-}$ and studied the electrochemical behavior of $[Sb_2W_{20}Fe_2O_{70}(H_2O)_6]^{8-}$ and its multilayer films fabricated onto the glassy carbon electrode (GCE) surface by layer-by-layer self-assembly.[17,18] In addition, the (organo)Ru-supported derivatives also have been presented; for example, Proust's group reported the (organo)Ru-supported tungstoantimonate $[Sb_2W_{20}O_{70}\{Ru(p\text{-cymene})\}_2]^{10-}$,[19] Kortz's group synthesized the (organo)Ru-supported tungstoantimonates and tungstobismuthates $[X_2W_{20}O_{70}(RuL)_2]^{10-}$ (X = Sb^{III}, Bi^{III}; L = benzene, *p*-cymene) and $[Bi_2W_{20}O_{70}(RuC_{10}H_{14})_2]^{10-}$.[20] It can be noticed that extended studies of X_2W_{22} or $X_2W_{20}M_2$ are still limited.

On the other hand, (bipyridine)ruthenium complexes have attracted much attention for their luminescence and

[a] College of Chemistry, State Key Laboratory of Supramolecular Structure and Materials, Jilin University, Changchun 130012, China
Fax: +86-431-85193421
E-mail: blh@jlu.edu.cn
wulx@jlu.edu.cn
[b] State Key Laboratory of Inorganic Synthesis and Preparative Chemistry, Jilin University, Changchun, 130012, China
[c] Electrochemistry Research Group, Dundalk Institute of Technology, Dundalk, County Louth, Ireland
E-mail: tim.mccormac@dkit.ie
[d] School of Engineering and Science, Jacobs University, P. O. Box 750561, 28725 Bremen, Germany
Fax: +49-421-200-3229
E-mail: u.kortz@jacobs-university.de

Supporting information for this article is available on the WWW under http://dx.doi.org/10.1002/ejic.200900590.

electrochemistry properties.[21,22] Trying to combine the favorable properties of a (bipyridine)ruthenium complex with those of Krebs-type sandwich POMs, we investigated the interaction of X_2W_{22} and $X_2W_{20}M_2$ with Rubpy in dmso/H_2O medium. More recently, our group described two examples of $[Ru^{II}(bpy)_3]_4[Sb_2W_{20}(OH)_2(dmso)_2O_{66}]\cdot16dmso\cdot2H_2O$ and $[Ru^{II}(bpy)_3]_2[Sb_2W_{20}Ru^{III}_2(H_2O)_2(dmso)_6O_{68}]\cdot3dmso$ based on X_2W_{22} and $X_2W_{20}M_2$.[23] Thus, the synthesis and structural characterization of novel Rubpy-containing POMs based on X_2W_{22} and $X_2W_{20}M_2$ remains of considerable importance for their further applications.

In 1970, Baker and Figgis formalized the class of Keggin-type heteropolyanions as $[(Y^{y-})M^{m+}O_5X^{x+}O_4(W \text{ or } Mo)_{11}O_{30}]^{(12-m-x+y)-}$, and they suggested that a large variety of ligands can function as Y.[24] Then Pope and co-workers systematically studied the Keggin system, and they were able to demonstrate ligand substitutions in aqueous or organic medium.[25] In 2000, Bi et al. systematically studied ligand replacement for Weakley-type POMs. These authors have shown that the external water molecules coordinated to the transition metal ions can be replaced by small inorganic or organic ligands.[26] The thus-formed products were only characterized by elemental analysis, IR and UV/Vis, but no crystal structures were obtained. Recently, large numbers of organic ligand-coordinated transition-metal-substituted POMs were synthesized by routine synthetic reactions or under hydrothermal conditions and structurally characterized.[27]

Recently, some structures of dmso-coordinated Ru/Os POMs have been reported by the groups of Kortz,[28,29] Neumann,[30] Proust[31], and Bi.[32] In 1997, Pope reported the (dmso)Rh-supported undecatungstophosphate $[(PO_4)W_{11}O_{35}\{Rh_2(OAc)_2(dmso)_2\}]^{5-}$.[33] In all of the above structures the dmso groups are coordinated to the Rh/Ru/Os centers through the sulfur atoms. Interestingly, our group recently showed that the dmso molecules are coordinated to the Ru^{III}/W centers through the oxygen atoms, indicating the novel bonding model of dmso molecules to the POM.[23] Following our research work, we studied the reactions of Rubpy with X_2W_{22} (X = Sb^{III} and Bi^{III}) and $X_2W_{20}Fe_2$ (X = Sb^{III} and Bi^{III}).

Herein, we report the syntheses, characterization, and crystal structures of four novel dmso-coordinated POMs, $[X_2W_{22}(dmso)_4O_{72}]^{4-}$ (X = Sb, **1**; Bi, **2**) and $[X_2W_{20}Fe_2(dmso)_8O_{68}]^{4-}$ (X = Sb, **3**; Bi, **4**). Obviously, (1) the polyanions **1** and **2** are second examples of dmso-coordinated polytungstates, that is, four dmso molecules are coordinated to the polytungstate frameworks; (2) the polyanions **3** and **4** exhibit the first examples of $Fe(dmso)_3$-supported POMs and second examples of dmso-coordinated transition-metal-substituted polytungstates.

Results and Discussion

Synthesis

The syntheses of **1a**–**4a** were accomplished by reactions of Rubpy with X_2W_{22}/$X_2W_{20}Fe_2$ in mixed solutions with dmso/H_2O (1:1, v/v). Therefore, the formation of **1a**–**4a** involves the substitution of hydroxy groups/oxygen atoms attached to W centers and water molecules coordinated to Fe centers by dmso molecules. In order to identify the crucial components/conditions for the formation of **1a**–**4a** we modified the reaction conditions systematically. For example, we tested if **1**–**4** can also be isolated from the mixed solutions with dmso/H_2O (1:1, v/v) in the absence of Rubpy, but the results indicated that no products were obtained. We also tested a two-step procedure: (1) reaction of X_2W_{22}/$X_2W_{20}Fe_2$ with Rubpy and isolation of Rubpy-X_2W_{22}/Rubpy-$X_2W_{20}Fe_2$; (2) redissolution of Rubpy-X_2W_{22}/Rubpy-$X_2W_{20}Fe_2$ in dmso with heating. This time we obtained **1a**–**4a** as based on IR spectroscopy. These observations allow the conclusion that the presence of Rubpy is crucial for the isolation of **1a**–**4a**. Interestingly, we can also prepare the osmium analogues of **1a**–**4a** by substituting $[Os(bpy)_3]^{2+}$ for $[Ru(bpy)_3]^{2+}$ as based on IR spectroscopy and cyclic voltammetry (CV).

Crystal Structures

Structural Features of $[X_2W_{22}(dmso)_4O_{72}]^{6-}$ (X = Sb, 1; Bi, 2)

The two polyoxoanions, $[Sb_2W_{22}(dmso)_4O_{72}]^{6-}$ (**1**) and $[Bi_2W_{22}(dmso)_4O_{72}]^{6-}$ (**2**), are isostructural. They consist of two $[B\text{-}\beta\text{-}XW_9O_{33}]^{9-}$ (X = Sb^{III}, Bi^{III}) moieties linked by two WO(dmso) and two WO_2(dmso) groups resulting in a sandwich-type structure with idealized C_2 symmetry (see Figure 1). This structural type was firstly reported by Krebs et al. for the sodium salt of $[X_2W_{22}O_{74}(OH)_2]^{12-}$ (X_2W_{22}) (X = Sb^{III}, Bi^{III}),[11,12] in which two $[B\text{-}\beta\text{-}XW_9O_{33}]^{9-}$ fragments are connected by two WO_2 and two WO_2(OH) groups. Comparison of the structures of **1** and **2** with that of X_2W_{22} indicates that dmso groups replace the oxygen atoms of WO_2 and hydroxy group of WO_2(OH) leading to dmso-coordinated polytungstates.

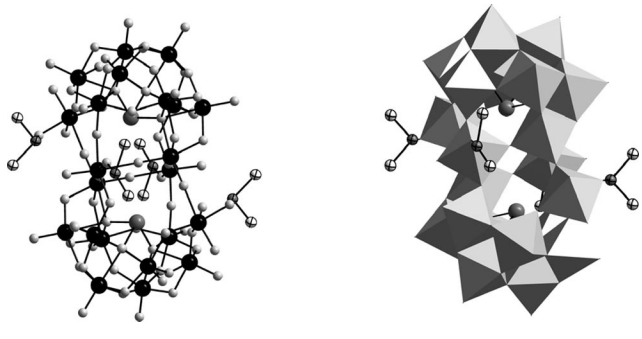

Figure 1. Ball-and-stick (left) and polyhedral (right) representations of **1** and **2**. Color code: tungsten (black ball), antimony/bismuth (dark gray ball), oxygen (light gray ball), sulfur (dark gray ball unfilled), and carbon (light gray ball unfilled). The WO_6 octahedra are gray. No hydrogen atoms shown for clarity.

Recently, our group reported on the first dmso-coordinated heteropolytungstate $[Sb_2W_{20}(OH)_2(dmso)_2O_{66}]^{8-}$,[23a] which is composed of two $[B\text{-}\beta\text{-}XW_9O_{33}]^{9-}$ units linked by

two WO(dmso) groups. In our case of **1** and **2**, the same WO(dmso) groups were also observed. In addition, the novel WO_2(dmso) groups were found in **1** and **2**, as shown in Figure 2. The atom W11 is bound to six oxygen atoms: three μ_2-oxo groups (O9, O31, O34) from two [*B*-*β*-$XW_9O_{33}]^{9-}$ units, two terminal oxygen atoms (O35 and O36), and one oxygen atom (O37) from the terminal dmso ligand for **1** and **2**. The W11–O bond lengths are in the expected range of around 1.717–2.215 Å [W11–O(T) 1.717(15)–1.738(15), W11–O(W) 1.829(11)–2.215(14), W11–O(S), 2.079(15) Å] for **1** and 1.714–2.209 Å [W11–O(T) 1.714(15)–1.732(11), W11–O(W) 1.908(11)–2.209(9), W11–O(S) 2.090(12) Å] for **2**. Comparison of the terminal W11–OT bond lengths in **1** and **2** with those in $[X_2W_{22}O_{74}(OH)_2]^{12-}$ (X = Sb^{III}, Bi^{III})[11,12] suggests that two W11–OT bond lengths in **1** and **2** do not indicate any hydroxy groups. This observation allows the conclusion that the two protonated W–OH groups in $[X_2W_{22}O_{74}(OH)_2]^{12-}$ (X = Sb^{III}, Bi^{III}) are replaced by two dmso groups resulting in the other two W–dmso bonds. Considering the above discussions indicates that a total of four dmso groups are coordinated to the X_2W_{22} framework, which reveals another novel bonding model.

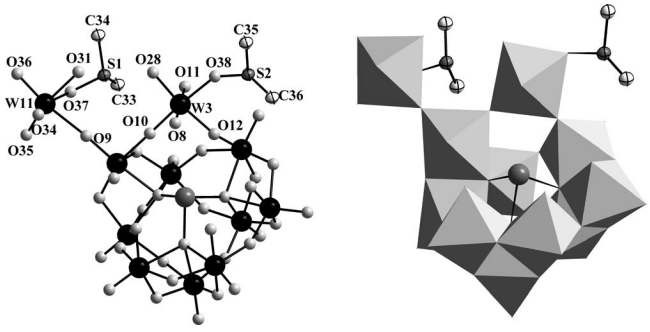

Figure 2. Ball-and-stick (left) and polyhedral (right) representations of the asymmetric unit of **1** and **2** with partial atom labeling. The color code is the same as in Figure 1.

Bond valence sum calculations[34] indicate that there are no protonation sites on **1** and **2**, and therefore the charge of the polyanions **1** and **2** must be –6. In the solid state the negative charges of **1** and **2** are balanced by two [Ru(bpy)$_3$]$^{2+}$ cations and two sodium ions, respectively. For **1** and **2** two sodium ions could not be detected by single-crystal XRD, probably due to disorder. However, the complete chemical composition was verified by elemental analysis.

Structural Features of [$X_2W_{20}Fe_2(dmso)_8O_{68}$]$^{4-}$ (X = Sb, 3; Bi, 4)

Single-crystal X-ray analyses on **3a** and **4a** revealed that **3** and **4** are composed of the usual $X_2W_{20}Fe_2$ Krebs-type POM frameworks, but unexpectedly they contain several dmso groups. More precisely, eight dmso groups are attached to **3** and **4** (see Figures 3 and 4). Six of the eight dmso groups are coordinated to the two Fe centers through Fe–O–S(CH$_3$)$_2$ bonds, and the other two dmso ligands are bound to the two tungsten atoms linking the two (*B*-*β*-XW_9O_{33}) units through W–O–S(CH$_3$)$_2$ bonds. Bonding of dmso to tungsten atoms of the polyanion framework has been observed in $[Sb_2W_{20}(OH)_2(dmso)_2O_{66}]^{8-}$ and $[Sb_2W_{20}Ru^{III}_2(H_2O)_2(dmso)_6O_{68}]^{4-}$ reported recently by our group.[23]

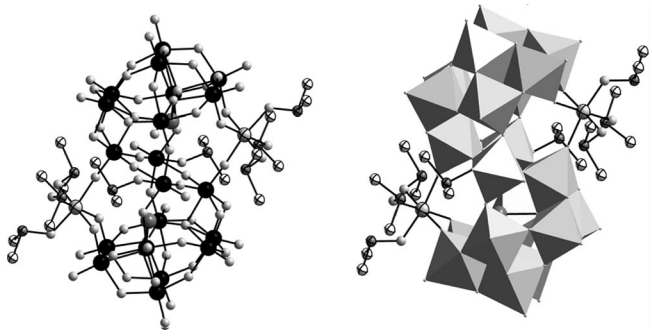

Figure 3. Ball-and-stick (left) and polyhedral (right) representations of **3** and **4**. Color code: tungsten (black ball), antimony/bismuth (dark gray ball), oxygen (light gray ball), iron (large light gray ball unfilled), sulfur (dark gray ball unfilled), and carbon (small light gray ball unfilled). The WO_6 octahedra are gray. No hydrogen atoms shown for clarity.

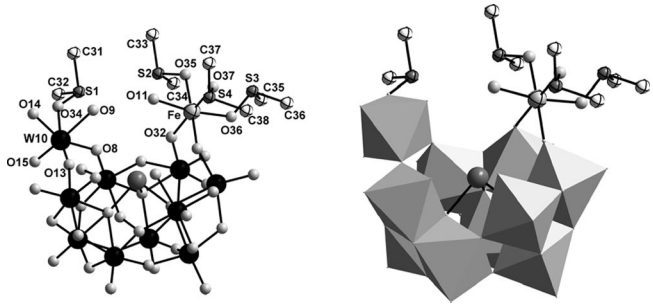

Figure 4. Ball-and-stick (left) and polyhedral (right) representations of the asymmetric unit of **3** and **4** with partial atom labeling. The color code is the same as in Figure 3.

In the previously reported (dmso)Ru^{II}/(dmso)Os^{II}-supported POMs the dmso ligands were always bound to the Ru^{II}/Os^{II} centers via the sulfur atoms.[28–32] Recently, our group reported on a (dmso)Ru^{III}-supported tungstoantimonate, in which the dmso ligands are bound to the Ru^{III} centers through the oxygen atoms. Interestingly, the same coordinating model was observed in **3** and **4**, namely, all dmso molecules are bound to the Fe^{III} centers through the oxygen atoms. This is in agreement with hard/soft acid–base principles.[35]

Each Fe center in **3** and **4** is coordinated by six oxo ligands, three μ_2-oxo groups of the tungsten–oxo frameworks and three oxo groups of the terminal dmso ligands. The Fe–O bond lengths are in the expected range of around 1.951–2.039 Å [Fe–O(W) 1.951(8)–2.005(8) Å, Fe–O(S) 2.005(8)–

2.039(8) Å] for **3** and 1.954–2.039 Å [Fe–O(W) 1.954(10)–2.024(9), Fe–O(S) 1.987(11)–2.039(12) Å] for **4**, respectively. Interestingly, the coordinating model of the Fe centers in **3** and **4** is very different from that of the Ru^{III} centers in $[Sb_2W_{20}Ru^{III}_2(H_2O)_2(dmso)_6O_{68}]^{4-}$, in which each Ru center is coordinated by three μ_2-oxo groups from the tungsten–oxo frameworks, two oxo groups from the terminal dmso ligands and a terminal water molecule.[23b]

Bond valence sum calculations[34] indicate that there are no protonation sites on **3** and **4**, and therefore the charge of the polyanions **3** and **4** must be –4. In the solid state, the negative charge of **3** and **4** is balanced by two $[Ru(bpy)_3]^{2+}$ cations, located by X-ray diffraction. Elemental analyses of **3a** and **4a** confirmed the chemical composition.

IR Spectra

IR spectra for **1a**–**4a** compared with those of Na-X_2W_{22} and KNa-$X_2W_{22}Fe_2$ are shown in Figures S1–S8 (see Supporting Information).

The following points can be drawn from the IR spectra: (1) Most of the characteristic vibrational frequencies for **1a**–**4a** increase compared with those of Na-X_2W_{22} and KNa-$X_2W_{22}Fe_2$, which is attributed to the decrease of the negative charges of the polyanions **1**–**4**. (2) The part of stretching vibrational frequencies of W–O_c–W and W–O_b–W in Na-X_2W_{22} and KNa-$X_2W_{22}Fe_2$ are split into two peaks in **1a**–**4a** due to the coordination of dmso ligands to the polyanion frameworks. (3) The expected S–O stretching vibrations of dmso molecules at ca. 1020 and ca. 1120 cm^{-1} are observed. (4) The IR spectra for **1a**–**4a** are similar to each other. (5) The IR spectra of **1a**–**4a** are very similar to their precursors Na-X_2W_{22}/KNa-$X_2W_{22}Fe_2$[11,12] and $Ru(bpy)_3Cl_2$[36] superimposed on each other, which implies that the Krebs-type POM frameworks are maintained in compounds **1a**–**4a**.

Electrochemistry

CV studies on **1a**–**4a** were performed in dmso/H_2SO_4 medium. The voltammogram of **1a** displays three redox waves at +1.00, –0.41, and –0.51 V, as shown in Figure 5. The first wave is a one-electron process, assigned to the $Ru^{3+/2+}$ couple; the second and third waves are multi-electron processes attributed to the redox reaction of the tungsten–oxo framework for tungstoantimonate. As expected, this voltammogram is very similar to that of Na-Sb_2W_{22}, as shown in Figure S9 at the same pH (see Supporting Information). The voltammogram of **2a** also displays three redox waves at +1.00, –0.44, and –0.56 V, as shown in Figure 6. The first redox wave is essentially identical with that of **1a**, and the second and third waves are multi-electron processes assigned to the redox reaction of the tungsten–oxo framework for tungstobismuthate, which is observed in the voltammogram of Na-Bi_2W_{22}, as shown in Figure S10 at the same pH (see Supporting Information).

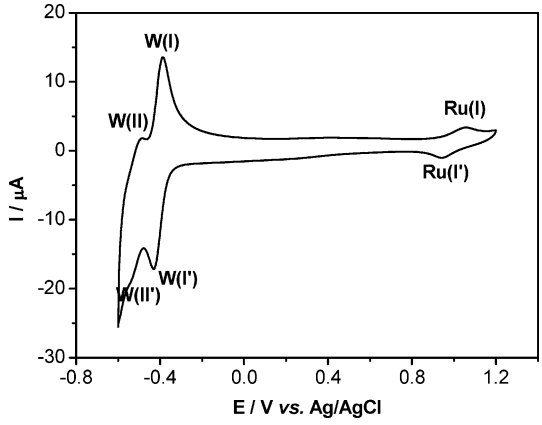

Figure 5. Cyclic voltammogram of 1.0 mM **1a** in dmso + 0.01 M Bu_4NPF_6 at pH = 2.0 at a bare GCE with scan rate 50 mV s^{-1}.

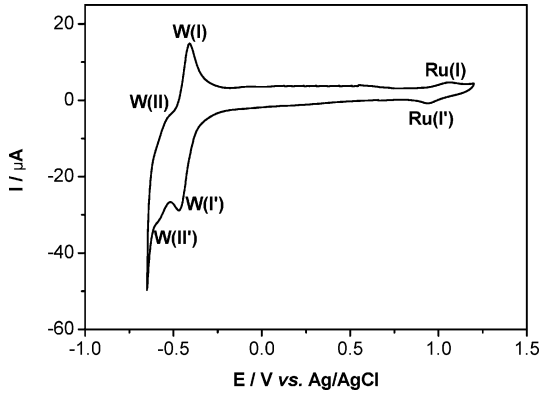

Figure 6. Cyclic voltammogram of 1.0 mM **2a** in dmso + 0.01 M Bu_4NPF_6 at pH = 2.0 at a bare GCE with scan rate 50 mV s^{-1}.

The voltammogram of **3a** displays five redox waves at +1.11, 0.31, 0.13, –0.37, and –0.47 V, as shown in Figure 7. The first wave is a one-electron process, assigned to the $Ru^{3+/2+}$ couple; the second and third waves are also one-electron processes, assigned to the $Fe^{3+/2+}$ couples, whereas the latter two waves are multi-electron processes attributed to the redox reaction of the tungsten–oxo framework for

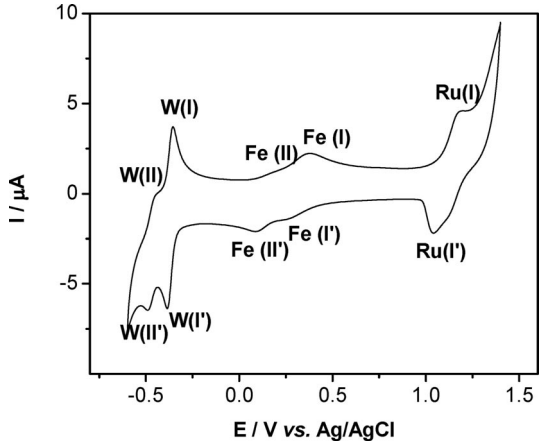

Figure 7. Cyclic voltammogram of 0.45 mM **3a** in dmso + 0.01 M Bu_4NPF_6 at pH = 1.7 at a bare GCE with scan rate 50 mV s^{-1}.

tungstoantimonate. As expected, this voltammogram is slightly different from that of $KNa\text{-}Sb_2W_{20}Fe_2$ in a buffer solution at the same pH (see Supporting Information, Figure S11), because the coordination of dmso molecules to the Fe centers results in a splitting of the Fe waves.[18,37] However, the voltammogram of **4a** displays four redox waves at +1.11, 0.33, 0.14, and –0.35 V, as shown in Figure 8. The first three redox waves are essentially identical with those of **3a**, and the fourth wave is a multi-electron process assigned to the redox reaction of the tungsten–oxo framework for tungstobismuthate (see Supporting Information, Figure S12).

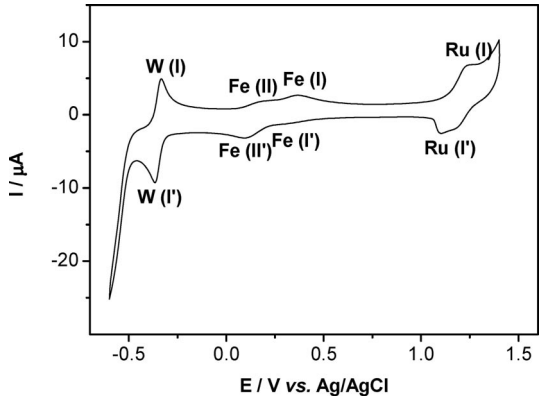

Figure 8. Cyclic voltammogram of 0.45 mM **4a** in dmso + 0.01 M Bu_4NPF_6 at pH = 1.7 at a bare GCE with scan rate 50 mV s^{-1}.

Thermal Analysis

Thermogravimetric analyses (TGA) have been performed for **1a** and **2a** between 20 and 900 °C and for **3a** and **4a** between 30 and 900 °C. All compounds show a continuous weight-loss process (see Supporting Information, Figures S13–S16), which corresponds to the removal of water molecules, dmso molecules including all noncoordinated and coordinated ones and 2,2′-bipyridyl ligands to the ruthenium atoms. The thermogravimetric (TG) curves of **1a**–**4a** show total weight losses of ca. 23.2, 22.5, 28.8, and 28.1% from the measurement temperature to 800 °C (calcd. ca. 22.3, 21.8, 31.7, and 31.1%), respectively. Thus, it can be seen that the total weight losses are fairly consistent with the calculated values.

Powder X-ray Diffraction Patterns

In order to verify the phase purity of the compounds **1a**–**4a**, we performed powder X-ray diffraction (PXRD) of **1a**–**4a** at room temperature. The PXRD patterns of **1a**–**4a** are shown in Figures S17–S20 (see Supporting Information). It can be seen that the diffraction peaks for compounds **1a**–**4a** of both simulated and experimental patterns match well in key positions, indicating the good phase purity of **1a**–**4a**.

Conclusions

We have synthesized four novel tris(bipyridine)ruthenium(II) salts of dmso-coordinated tungstoantimonate/tungstobismuthate and Fe-substituted tungstoantimonate/tungstobismuthate. These compounds are of interest for several reasons: (1) For **1a** and **2a**, four dmso molecules are coordinated to the polytungstate frameworks through W–O–$S(CH_3)_2$ bonds. They are the second examples of dmso-coordinated polytungstate; (2) for **3a** and **4a**, they not only contain dmso molecules coordinated to W^{VI} centers but also to Fe centers through Fe–O–$S(CH_3)_2$ bonds. They are also the second examples of dmso-coordinated transition-metal-substituted polytungstates; (3) **3a** and **4a** represent the first examples of $Fe(dmso)_3$-supported POMs; (4) **3a** and **4a** add new members to (organo)metal-containing POMs and substituted-type tungstoantimonates/tungstobismuthates in particular; (5) the electrochemical behaviors of compounds **1a** and **2a** show the expected redox couples of the Ru and W centers; (6) the electrochemical behaviors of compounds **3a** and **4a** show the expected redox couples of the Ru, Fe, and W centers; (7) the structures of **1a**–**4a** allow for a multitude of studies including organic catalysis, multifunctional electrocatalysis and solid-state ECL detection. Some of this work is currently in progress, and the results will be reported in due time.

Experimental Section

Materials and Methods: $Na_{12}[Sb_2W_{22}O_{74}(OH)_2]$ ($Na\text{-}Sb_2W_{22}$), $Na_{12}[Bi_2W_{22}O_{74}(OH)_2]$ ($Na\text{-}Bi_2W_{22}$), $K_6NaH[Sb_2W_{20}Fe_2O_{70}(H_2O)_6]$ ($KNa\text{-}Sb_2W_{20}Fe_2$), and $K_6NaH[Bi_2W_{20}Fe_2O_{70}(H_2O)_6]$ ($KNa\text{-}Bi_2W_{20}Fe_2$) were synthesized according to the literature and characterized by IR spectra.[11,12] All other reagents were used as purchased without further purification. Deionized water was used throughout. Elemental analyses (Sb, Bi, W, Ru, Fe, Na) were performed with an Inductively Coupled Plasma Optical Emission Spectrometer (ICP-OES, ICAP 6000, Thermo, USA). Elemental analyses (C, H, N, and S) were performed with a Flash EA1112 from ThermoQuest Italia S.P.A. IR spectra of **1a**–**4a** were recorded in the range 400–4000 cm^{-1} with a Bruker IFS-66V Fourier transform infrared spectrometer by using KBr pellets. Thermogravimetric analyses of **1a** and **2a** were carried out with a TA Instruments SDT Q600 thermobalance. The thermal gravimetric analyses of **3a** and **4a** were carried out with a TGA Q500 V20.8 Build 34 thermal analysis system. X-ray powder diffraction was performed with a Siemens D5005 diffractometer with graphite-filtered Cu-K_a radiation. Electrochemical measurements were carried out with a CHI 660C electrochemical workstation at room temperature under nitrogen. A three-electrode electrochemical cell was used with a GCE as the working electrode, a platinum wire as the counter and an Ag/AgCl reference electrode. Formal potentials (E_f) were estimated as average values of anodic (E_{pa}) and cathodic (E_{pc}) peak potentials, i.e., $E_f = (E_{pa} + E_{pc})/2$.

Synthesis of $[Ru(bpy)_3]_2Na_2[Sb_2W_{22}(dmso)_4O_{72}]\cdot 4dmso\cdot 4H_2O$ (1a): Compound **1a** was synthesized by addition of $Ru(bpy)_3Cl_2$ (0.5 g, 0.67 mmol) and $Na\text{-}Sb_2W_{22}$ (1.0 g, 0.16 mmol) to dmso/H_2O (20 mL) (1:1, v/v), and the pH was adjusted to 2 with 1.0 M H_2SO_4. The solution was heated to 80 °C for 1 h and then filtered after it had cooled down. Single crystals suitable for X-ray analysis were

obtained by slow concentration of the filtrate at room temperature. Yield: 0.32 g (28%). $C_{76}H_{104}N_{12}Na_2O_{84}Ru_2S_8Sb_2W_{22}$ (7322.31): calcd. C 12.5, H 1.4, N 2.3, Na 0.6, Ru 2.7, S 3.5, Sb 3.3, W 55.2; found C 13.1, H 1.9, N 2.6, Na 0.7, Ru 2.4, S 3.9, Sb 3.3, W 54.6. IR: $\tilde{\nu}_{max}$ = 1462 (w), 1445 (w), 1424 (w), 1311 (w), 1271 (w), 1242 (w), 1161 (w), 1118 (w), 1063 (sh), 1025 (w), 959 (s), 878 (sh), 855 (m), 815 (s), 766 (s), 743 (sh) cm^{-1}.

Synthesis of $[Ru(bpy)_3]_2Na_2[Bi_2W_{22}(dmso)_4O_{72}]\cdot 4dmso\cdot 4H_2O$ (2a): Compound **2a** was synthesized by addition of $Ru(bpy)_3Cl_2$ (0.5 g, 0.67 mmol) and Na-Bi_2W_{22} (1.0 g, 0.15 mmol) to dmso/H_2O (20 mL) (1:1, v/v), and the pH was adjusted to 2 with 1.0 M H_2SO_4. The solution was heated to 80 °C for 1 h and then filtered after it had cooled down. Single crystals suitable for X-ray analysis were obtained by slow concentration of the filtrate at room temperature. Yield: 0.37 g (33%). $C_{76}H_{104}Bi_2N_{12}Na_2O_{84}Ru_2S_8W_{22}$ (7496.76): calcd. C 12.2, H 1.4, Bi 5.6, N 2.3, Na 0.6, Ru 2.7, S 3.4, W 54.0; found C 12.1, H 1.8, Bi 5.3, N 2.6, Na 0.7, Ru 2.5, S 3.7, W 53.8. IR: $\tilde{\nu}_{max}$ = 1462 (w), 1444 (w), 1421 (w), 1312 (w), 1268 (w), 1242 (w), 1161 (w), 1124 (w), 1066 (sh), 1023 (w), 957 (s), 875 (m), 847 (m), 809 (s), 766 (s), 731 (m) cm^{-1}.

Synthesis of $[Ru(bpy)_3]_2[Sb_2W_{20}Fe_2(dmso)_8O_{68}]\cdot 9dmso\cdot 12H_2O$ (3a): Compound **3a** was synthesized by addition of $Ru(bpy)_3Cl_2$ (0.5 g, 0.67 mmol) and KNa-$Sb_2W_{20}Fe_2$ (1.0 g, 0.17 mmol) to dmso/H_2O (20 mL) (1:1, v/v). The solution was heated to 80 °C for 1 h and then filtered after it had cooled down. Single crystals suitable for X-ray analysis were obtained by slow concentration of the filtrate at room temperature. Yield: 0.45 g (34%). $C_{94}H_{174}Fe_2N_{12}O_{97}Ru_2S_{17}Sb_2W_{20}$ (7803.81): calcd. C 14.4, H 2.2, Fe 1.4, N 2.1, Ru 2.6, S 6.9, Sb 3.1, W 47.1; found C 14.1, H 1.8, Fe 1.6, N 2.0, Ru 2.7, S 6.4, Sb 3.3, W 48.0. IR: $\tilde{\nu}_{max}$ = 1465 (w), 1445 (w), 1421 (w), 1312 (w), 1268 (w), 1242 (w), 1161 (w), 1124 (w), 1066 (sh), 1026 (w), 959 (s), 875 (m), 855 (m), 815 (s), 763 (s), 748 (sh), 731 (m) cm^{-1}.

Synthesis of $[Ru(bpy)_3]_2[Bi_2W_{20}Fe_2(dmso)_8O_{68}]\cdot 9dmso\cdot 12H_2O$ (4a): Compound **4a** was synthesized by addition of $Ru(bpy)_3Cl_2$ (0.5 g, 0.67 mmol) and KNa-$Bi_2W_{20}Fe_2$ (1.0 g, 0.17 mmol) to H_2O/dmso (20 mL) (1:1, v/v). The solution was heated to 80 °C for 1 h and then filtered after it had cooled down. Single crystals suitable for X-ray analysis were obtained by slow concentration of the filtrate at room temperature. Yield: 0.45 g (33%). $C_{94}H_{174}Bi_2Fe_2N_{12}O_{97}Ru_2S_{17}W_{20}$ (7978.27): calcd. C 14.2, H 2.2, Bi 5.3, Fe 1.4, N 2.1, Ru 2.5, S 6.8, W 46.1; found C 13.8, H 1.8, Bi 5.6, Fe 1.5, N 1.8, Ru 2.8, S 6.4, W 46.5. IR: $\tilde{\nu}_{max}$ = 1462 (w), 1445 (w), 1424 (w), 1312 (w), 1271 (w), 1242 (w), 1219 (w), 1161 (w), 1121 (w), 1066 (sh), 1023 (w), 953 (s), 870 (m), 847 (m), 809 (s), 768 (m), 737 (s) cm^{-1}.

X-ray Crystallography: Single crystals of compounds **1a** and **2a** were mounted on a Rigaku/MSC mercury diffractometer with graphite-monochromated Mo-K_α radiation (λ = 0.71073 Å) for indexing and intensity data collection at 293 K. Single crystals of compounds **3a** and **4a** were mounted on a Bruker X8 APEX II CCD diffractometer with kappa geometry and Mo-K_α radiation (λ = 0.71073 Å) for indexing and intensity data collection at 173 K. In both cases direct methods were used to solve the structures and to locate the heavy atoms (SHELXS97), and then the remaining atoms were found from successive difference maps (SHELXL97).[38] An absorption corrections was also performed.[39] Crystallographic data are summarized in Table 1. CCDC-737643 (for **1a**), -737644 (for **2a**), -645252 (for **3a**), and -645251 (for **4a**) contain the supplementary crystallographic data for this paper. These data can be obtained free of charge from The Cambridge Crystallographic Data Centre via www.ccdc.cam.ac.uk/data_request/cif.

Supporting Information (see footnote on the first page of this article): Fourier transform IR spectra of **1a**–**4a** and their precursors

Table 1. Crystal data and structure refinements for **1a**–**4a**.

	1a	**2a**	**3a**	**4a**
Empirical formula	$C_{76}H_{104}N_{12}Na_2O_{84}Ru_2S_8Sb_2W_{22}$	$C_{76}H_{104}Bi_2N_{12}Na_2O_{84}Ru_2S_8W_{22}$	$C_{94}H_{174}Fe_2N_{12}O_{97}Ru_2S_{17}Sb_2W_{20}$	$C_{94}H_{174}Bi_2Fe_2N_{12}O_{97}Ru_2S_{17}W_{20}$
Formula mass	7322.31	7496.76	7803.81	7978.27
Crystal size [mm]	0.16×0.15×0.15	0.12×0.11×0.10	0.14×0.13× 0.13	0.16×0.14×0.14
Crystal system	triclinic	triclinic	monoclinic	monoclinic
Space group	$P\bar{1}$	$P\bar{1}$	$P2_1/n$	$P2_1/n$
a [Å]	13.7388(11)	13.7122(9)	17.7305(15)	17.7507(13)
b [Å]	15.5440(13)	15.5612(11)	20.8302 (17)	20.7832(12)
c [Å]	20.6537(18)	20.6225(14)	25.0301 (17)	24.9676(13)
α [°]	71.8550(13)	72.1660(10)	90	90
β [°]	88.5910(14)	88.5730(10)	103.777(4)	103.882(2)
γ [°]	73.8550(13)	74.1660(10)	90	90
V [Å^3]	4016.8(6)	4021.7(5)	8978.4(12)	8941.9(10)
Z	1	1	2	2
T [K]	291(2)	291(2)	173(2)	173(2)
λ [Å]	0.71073	0.71073	0.71073	0.71073
F(000)	3264	3328	7184	7312
Parameters	982	990	1144	1079
$d_{calcd.}$ [mg m^{-3}]	3.009	3.077	2.887	2.963
μ [mm^{-1}]	16.378	18.207	13.658	15.377
Reflections (collected)	20474	20481	163534	116746
Reflections (unique)	13714	13660	15724	14453
Reflections (observed)	9035	10173	11449	9346
GOF	0.938	0.978	1.136	1.009
R [$I>2\sigma(I)$][a]	0.0549	0.0595	0.0424	0.0500
R_w (all data)[b]	0.1348	0.1441	0.1081	0.1199

[a] $R = \Sigma||F_o| - |F_c||/\Sigma|F_o|$. [b] $Rw = [\Sigma w(F_o^2 - F_c^2)2/\Sigma w(F_o^2)^2]^{1/2}$.

Na-X_2W_{22} and KNa-$X_2W_{20}Fe_2$. CVs of precursors Na-X_2W_{22} and KNa-$X_2W_{20}Fe_2$. TGA curves of **1a**–**4a**. PXRD patterns of **1a**–**4a**.

Acknowledgments

This work was financially supported by the projects of National Basic Research Program (2007CB808003), the National Natural Science Foundation of China (20703019, 20731160002, 20973082), the 111 Project (B06009) for international cooperation, the Scientific Research Foundation for Returned Overseas Chinese Scholars, State Education Ministry (3C108K291412), the Science Foundation of Jilin University (421020070463) and the Technology of Jilin Province, China (20090592).

[1] a) T. R. Zhang, S. Q. Liu, D. G. Kurth, C. F. J. Faul, *Adv. Funct. Mater.* **2009**, *19*, 642–652; b) B. Hasenknopf, K. Micoine, E. Lacote, S. Thorimbert, M. Malacria, R. Thouvenot, *Eur. J. Inorg. Chem.* **2008**, 5001–5013; c) J. Li, I. Huth, L. M. Chamoreau, B. Hasenknopf, K. Micoine, E. Lacote, S. Thorimbert, M. Malacria, *Angew. Chem. Int. Ed.* **2009**, *48*, 2035–2038.

[2] a) S. Y. Yin, H. Sun, Y. Yan, W. Li, L. X. Wu, *J. Phys. Chem. B* **2009**, *113*, 2355–2364; b) W. Qi, H. L. Li, L. X. Wu, *J. Phys. Chem. B* **2008**, *112*, 8257–8263; c) H. Sun, W. F. Bu, Y. C. Li, H. L. Li, L. X. Wu, C. Q. Sun, B. Dong, R. F. Doo, L. F. Chi, A. Schaefer, *Langmuir* **2008**, *24*, 4693–4699; d) W. Li, S. Y. Yin, J. F. Wang, L. X. Wu, *Chem. Mater.* **2008**, *20*, 514–522.

[3] a) J. P. Wang, J. W. Zhao, P. T. Ma, J. C. Ma, L. P. Yang, M. X. Li, J. Y. Niu, *Chem. Commun.* **2009**, 2362–2364; b) J. P. Wang, P. T. Ma, Y. Shen, J. Y. Niu, *Cryst. Growth Des.* **2008**, *8*, 3130–3133; c) J. W. Zhao, S. T. Zheng, Z. H. Li, G. Y. Yang, *Dalton Trans.* **2009**, 1300–1306; d) J. W. Zhao, J. Zhang, Y. Song, S. T. Zheng, G. Y. Yang, *Eur. J. Inorg. Chem.* **2008**, 3809–3819; e) Y. G. Li, L. Xu, G. G. Gao, N. Jiang, H. Liu, F. Y. Li, Y. Y. Yang, *CrystEngComm* **2009**, *11*, 1512–1514; f) A. Michailovski, F. Hussain, B. Spingler, J. Wagler, G. R. Patzke, *Cryst. Growth Des.* **2009**, *9*, 755–765.

[4] a) A. H. Ismail, M. H. Dickman, U. Kortz, *Inorg. Chem.* **2009**, *48*, 1559–1565; b) C. Pichon, P. Mialane, A. Dolbecq, J. Marrot, E. Riviere, B. S. Bassil, U. Kortz, B. Keita, L. Nadjo, F. Secheresse, *Inorg. Chem.* **2008**, *47*, 11120–11128; c) E. V. Chubarova, M. H. Dickman, B. Keita, L. Nadjo, F. Miserque, M. Mifsud, I. W. C. E. Arends, U. Kortz, *Angew. Chem. Int. Ed.* **2008**, *47*, 9542–9546; d) S. S. Mal, M. H. Dickman, U. Kortz, *Chem. Eur. J.* **2008**, *14*, 9851–9855.

[5] a) Y. V. Geletii, B. Botar, P. Kögerler, D. A. Hillesheim, D. G. Musaev, C. L. Hill, *Angew. Chem. Int. Ed.* **2008**, *47*, 3896–3899; b) R. Cao, T. M. Anderson, D. A. Hillesheim, P. Kögerler, K. I. Hardcastle, C. L. Hill, *Angew. Chem. Int. Ed.* **2008**, *47*, 9380–9382; c) S. G. Mitchell, S. Khanra, H. N. Miras, T. Boyd, D. L. Long, L. Cronin, *Chem. Commun.* **2009**, 2712–2714; d) H. N. Miras, J. Yan, D. L. Long, L. Cronin, *Angew. Chem. Int. Ed.* **2008**, *47*, 820–8423; e) C. P. Pradeep, D. L. Long, C. Streb, L. Cronin, *J. Am. Chem. Soc.* **2008**, *130*, 14946–14947; f) S. G. Mitchell, D. Gabb, C. Ritchie, N. Hazel, D. L. Long, L. Cronin, *CrystEngComm* **2009**, *11*, 36–39.

[6] a) L. H. Bi, G. F. Hou, B. Li, L. X. Wu, U. Kortz, *Dalton Trans.* **2009**, 6345–6353; b) L. H. Bi, G. F. Hou, L. X. Wu, U. Kortz, *CrystEngComm* **2009**, *11*, 1532–1535; c) L. H. Bi, B. Li, L. X. Wu, Y. Y. Bao, *Inorg. Chim. Acta* **2009**, *362*, 3309–3313; d) L. H. Bi, E. V. Chubarova, N. H. Nsouli, M. H. Dickman, U. Kortz, B. Keita, L. Dadjo, *Inorg. Chem.* **2006**, *45*, 8575–8583; e) L. H. Bi, U. Kortz, B. Keita, L. Nadjo, L. Daniels, *Eur. J. Inorg. Chem.* **2005**, 3034–3041.

[7] a) Y. Y. Yang, L. Xu, G. G. Gao, F. Y. Li, X. Z. Liu, W. H. Guo, *Eur. J. Inorg. Chem.* **2009**, 1460–1463; b) G. G. Gao, F. Y. Li, L. Xu, X. Z. Liu, Y. Y. Yang, *J. Am. Chem. Soc.* **2008**, *130*, 10838–10839; c) C. Y. Sun, S. X. Liu, D. D. Liu, K. Z. Shao, Y. H. Ren, Z. M. Su, *J. Am. Chem. Soc.* **2009**, *131*, 1883–1888; d) Y. Q. Lan, S. L. Li, K. Z. Shao, X. L. Wang, X. R. Hao, Z. M. Su, *Dalton Trans.* **2009**, 940–947; e) A. X. Tian, J. Ying, J. Peng, J. Q. Sha, H. J. Pang, P. P. Zhang, Y. Chen, M. Zhu, Z. M. Su, *Inorg. Chem.* **2009**, *48*, 100–110; f) Q. Wu, Y. G. Li, Y. H. Wang, R. Clérac, Y. Lu, E. B. Wang, *Chem. Commun.* **2009**, 5743–5745.

[8] a) Y. F. Song, N. McMillan, D. L. Long, S. Kane, J. Malm, M. O. Riehle, C. P. Pradeep, N. Gadegaard, L. Cronin, *J. Am. Chem. Soc.* **2009**, *131*, 1340–1341; b) E. F. Wilson, H. Abbas, B. J. Duncombe, C. Streb, D. L. Long, L. Cronin, *J. Am. Chem. Soc.* **2008**, *130*, 13876–13884; c) C. P. Pradeep, D. L. Long, G. N. Newton, Y. F. Song, L. Cronin, *Angew. Chem. Int. Ed.* **2008**, *47*, 4388–4391.

[9] a) U. Kortz, A. Müller, J. van Slageren, J. Schnack, N. S. Dalal, M. Dressel, *Coord. Chem. Rev.* **2009**, *253*, 2315–2327; b) J. W. Zhao, C. M. Wang, J. Zhang, S. T. Zheng, G. Y. Yang, *Chem. Eur. J.* **2008**, *14*, 9223–9239; c) J. Thiel, C. Ritchie, C. Streb, D. L. Long, L. Cronin, *J. Am. Chem. Soc.* **2009**, *131*, 4180–4181.

[10] J. Fischer, L. Ricard, R. Weiss, *J. Am. Chem. Soc.* **1976**, *98*, 3050–3052.

[11] M. Bösing, I. Loose, H. Pohlmann, B. Krebs, *Chem. Eur. J.* **1997**, *3*, 1232–1237.

[12] I. Loose, E. Droste, M. Bösing, H. Pohlmann, M. H. Dickman, C. Rosu, M. T. Pope, B. Krebs, *Inorg. Chem.* **1999**, *38*, 2688–2694.

[13] a) L. H. Bi, M. H. Dickman, U. Kortz, *CrystEngComm* **2009**, *11*, 965–966; b) L. H. Bi, M. Reicke, U. Kortz, B. Keita, L. Nadjo, R. J. Clark, *Inorg. Chem.* **2004**, *43*, 3915–3920; c) F. Hussain, M. Reicke, U. Kortz, *Eur. J. Inorg. Chem.* **2004**, 2733–2738; d) U. Kortz, M. G. Savelieff, B. S. Bassil, B. Keita, L. Nadjo, *Inorg. Chem.* **2002**, *41*, 783–789; e) U. Kortz, N. K. Al-Kassem, M. G. Savelieff, N. A. Al Kadi, M. Sadakane, *Inorg. Chem.* **2001**, *40*, 4742–4749.

[14] J. P. Wang, P. T. Ma, J. Li, H. Y. Niu, J. Y. Niu, *Chem. Asian J.* **2008**, *3*, 822–833.

[15] L. F. Chen, K. Zhu, L. H. Bi, A. Suchopar, M. Reicke, G. Mathys, H. Jaensch, U. Kortz, R. M. Richards, *Inorg. Chem.* **2007**, *46*, 8457–8459.

[16] L. H. Bi, B. Li, L. X. Wu, *J. Coord. Chem.* **2009**, *62*, 531–539.

[17] L. H. Bi, B. Li, Y. Y. Bao, L. X. Wu, *Inorg. Chim. Acta* **2009**, *362*, 1600–1604.

[18] L. H. Bi, T. McCormac, S. Beloshapkin, E. Dempsey, *Electroanalysis* **2008**, *20*, 38–46.

[19] D. Laurencin, R. Villanneau, P. Herson, R. Thouvenot, Y. Jeannin, A. Proust, *Chem. Commun.* **2005**, 5524–5526.

[20] L. H. Bi, G. Al-Kadamany, E. V. Chubarova, M. H. Dickman, L. F. Chen, D. S. Gopala, R. M. Richards, B. Keita, L. Nadjo, H. Jaensch, G. Mathys, U. Kortz, *Inorg. Chem.* **2009**, online; DOI: 10.1021/ic9009306.

[21] a) M. M. Richter, *Chem. Rev.* **2004**, *104*, 3003–3036; b) A. Arora, J. C. T. Eijkel, W. E. Morf, A. Manz, *Anal. Chem.* **2001**, *73*, 3282–3288.

[22] X. P. Sun, Y. Du, L. X. Zhang, S. J. Dong, E. K. Wang, *Anal. Chem.* **2007**, *79*, 2588–2592.

[23] a) L. H. Bi, B. Li, L. X. Wu, *Inorg. Chem. Commun.* **2008**, *11*, 1184–1186; b) L. H. Bi, B. Li, S. Bi, L. X. Wu, *J. Solid State Chem.* **2009**, *182*, 1401–1407.

[24] L. C. M. Baker, J. S. Figgis, *J. Am. Chem. Soc.* **1970**, *92*, 3794–3797.

[25] a) J. L. Samonte, M. T. Pope, *Can. J. Chem.* **2001**, *79*, 802–808; b) H. Y. Woo, H. S. So, M. T. Pope, *J. Am. Chem. Soc.* **1996**, *118*, 621–626; c) K. Piepgrass, M. T. Pope, *J. Am. Chem. Soc.* **1989**, *111*, 753–754.

[26] a) L. H. Bi, R. D. Huang, J. Peng, E. B. Wang, Y. H. Wang, C. W. Hu, *J. Chem. Soc., Dalton Trans.* **2001**, 121–129; b) L. H. Bi, E. B. Wang, J. Peng, R. D. Huang, L. Xu, C. W. Hu, *Inorg. Chem.* **2000**, *39*, 671–679.

[27] a) H. Liu, C. Qin, Y. G. Wei, L. Xu, G. G. Gao, F. Y. Li, X. S. Qu, *Inorg. Chem.* **2008**, *47*, 4166–4172; b) S. Reinoso, M. H. Dickman, U. Kortz, *Eur. J. Inorg. Chem.* **2009**, 947–953; c) X. K. Fang, P. Kögerler, L. Lsaacs, S. Uchida, N. Mizuno, *J. Am. Chem. Soc.* **2009**, *131*, 432–433.
[28] a) L. H. Bi, S. S. Mal, N. H. Nsouli, M. H. Dickman, U. Kortz, S. Nellutla, N. S. Dalal, M. Prinz, G. Hofmann, M. Neumann, *J. Cluster Sci.* **2008**, *19*, 259–273; b) M. Sadakane, D. Tsukuma, M. H. Dickman, B. Bassil, U. Kortz, M. Higashijima, W. Ueda, *Dalton Trans.* **2006**, 4271–4276.
[29] a) L. H. Bi, F. Hussain, U. Kortz, M. Sadakane, M. H. Dickman, *Chem. Commun.* **2004**, 1420–1421; b) L. H. Bi, U. Kortz, B. Keita, L. Nadjo, *Dalton Trans.* **2004**, 3184–3190; c) L. H. Bi, M. H. Dickman, U. Kortz, I. Dix, *Chem. Commun.* **2005**, 3962–3964.
[30] A. M. Khenkin, L. J. W. Shimon, R. Neumann, *Inorg. Chem.* **2003**, *42*, 3331–3339.
[31] a) D. Laurencin, R. Villanneau, H. Gerard, A. Proust, *J. Phys. Chem. A* **2006**, *110*, 6345–6355; b) D. Laurencin, A. Proust, H. Gerard, *Inorg. Chem.* **2008**, *47*, 7888–7893.
[32] L. H. Bi, B. Li, L. X. Wu, K. Z. Shao, Z. M. Su, *J. Solid State Chem.* **2009**, *182*, 83–88.
[33] X. Y. Wei, M. H. Dickman, M. T. Pope, *Inorg. Chem.* **1997**, *36*, 130–131.
[34] I. D. Brown, D. Altermatt, *Acta Crystallogr., Sect. B* **1985**, *41*, 244–247.
[35] S. Ahrland, J. Chatt, N. R. Davies, *Quart. Rev. Chem. Soc.* **1958**, *12*, 265–270.
[36] L. H. Bi, W. H. Zhou, H. Y. Wang, S. J. Dong, *Electroanalysis* **2008**, *20*, 996–1001.
[37] K. Foster, L. H. Bi, T. McCormac, *Electrochim. Acta* **2008**, *54*, 868–875.
[38] G. M. Sheldrick, *SHELXS-97* and *SHELXL-97*, University of Göttingen, Göttingen, Germany, **1997**.
[39] G. M. Sheldrick, *SADABS*, University of Göttingen, Germany, **1996**.

Received: June 26, 2009
Published Online: October 23, 2009

